EDGEWOOD
RESEARCH DEVELOPMENT & ENGINEERING CENTER
U.S. ARMY CHEMICAL AND BIOLOGICAL DEFENSE COMMAND

ERDEC-TR-173

VAPOR DETECTION SENSITIVITY AS A FUNCTION OF OPTICAL RESOLUTION FOR A SINGLE LORENTZIAN BAND

Dennis F. Flanigan

RESEARCH AND TECHNOLOGY DIRECTORATE

July 1994

Aberdeen Proving Ground, MD 21010-5423

Disclaimer

The findings in this report are not to be construed as an official Department of the Army position unless so designated by other authorizing documents.

REPORT DOCUMENTATION PAGE

Form Approved
OMB No. 0704-0188

1. AGENCY USE ONLY (Leave blank)	2. REPORT DATE	3. REPORT TYPE AND DATES COVERED
	1994 July	Final, 93 Dec - 94 Apr

4. TITLE AND SUBTITLE

Vapor Detection Sensitivity as a Function of Optical Resolution for a Single Lorentzian Band

5. FUNDING NUMBERS

PR-1O162622A553

6. AUTHOR(S)

Flanigan, Dennis F.

7. PERFORMING ORGANIZATION NAME(S) AND ADDRESS(ES)

DIR, ERDEC, ATTN: SCBRD-RTM, APG, MD 21010-5423

8. PERFORMING ORGANIZATION REPORT NUMBER

ERDEC-TR-173

9. SPONSORING / MONITORING AGENCY NAME(S) AND ADDRESS(ES)

10. SPONSORING / MONITORING AGENCY REPORT NUMBER

11. SUPPLEMENTARY NOTES

12a. DISTRIBUTION / AVAILABILITY STATEMENT

Approved for public release; distribution is unlimited.

12b. DISTRIBUTION CODE

13. ABSTRACT *(Maximum 200 words)*

The objective of this effort is twofold: to begin the development of a computer model for passive infrared (IR) remote sensing vapor detection systems and to provide guidance for the determination of optimum spectral resolution for the remote detection of organic vapors. The target bands are modeled as Lorentzian bands; this allows a fairly simple analytical approach. Several sensor models are compared including: a detector limited sensor model according to Wolfe, and 2 background limited incident photon (BLIP) models based on work by Wolfe and Kingston. The measures of sensitivity are signal to noise ratio (SNR), noise equivalent concentration pathlength (NECL) and noise equivalent ΔT (NEDT) all as a function of optical bandwidth. Signal to noise ratio, NECL and NEDT values are computed for a typical broad and narrow band associated with organophosphorus compounds. Additionally, the simulant, sulfur hexafluoride (SF_6) is evaluated. The results show that gains in sensitivity may be possible in existing remote sensors if the current optical resolution 4 cm^{-1}, is reduced to 8 cm^{-1} or 16 cm^{-1}, although this must be done carefully to ensure no loss in discrimination. It is clear that present systems are limited by detector technology. With true background limited performance and careful optimization to a particular problem, sensitivity improvements of 50 may be possible.

14. SUBJECT TERMS

D*	Infrared	Signal to noise
FTS	Detection	Fourier transform
XM21	Sensitivity	Optical resolution

15. NUMBER OF PAGES 28

16. PRICE CODE

17. SECURITY CLASSIFICATION OF REPORT	18. SECURITY CLASSIFICATION OF THIS PAGE	19. SECURITY CLASSIFICATION OF ABSTRACT	20. LIMITATION OF ABSTRACT
UNCLASSIFIED	UNCLASSIFIED	UNCLASSIFIED	UL

Blank

PREFACE

The work described in this report was authorized under Project No. 1O162622A553, CB Defense/General Investigation. This work was started in December 1993 and completed in April 1994.

The use of trade names or manufacturers' names in this report does not constitute an official endorsement of any commercial products. This report may not be cited for purposes of advertisement.

This report has been approved for release to the public. Registered users should request additional copies from the Defense Technical Information Center; unregistered users should direct such requests to the National Technical Information Service.

Acknowledgments

The author wishes to thank Avi Ben-David for many helpful discussions on Mathematica© and Tom Quinn for his help in understanding electronic bandwidth.

Blank

CONTENTS

LIST OF FIGURES

LIST OF TABLES

Blank

Vapor Detection Sensitivity as a Function of Optical Resolution for a Single Lorentzian Band

1. Introduction

Passive infrared spectroscopy, in many practical situations, produces marginal signals because of the small difference temperature (ΔT) between the target gas and the background. ΔT will range from as a little as a fraction of a °K to an unusually generous 20 °K.[1,2] When compared to a laboratory spectrometer where the source temperature may be well above 1000 °K it is easy to see why it is worthwhile to optimize the sensor resolution for a particular problem.

Spectral resolution has been a particularly controversial parameter.; it has been chosen for various reasons including: bandwidth of target gases, bandwidth of the atmospheric gases, and the always present tendency to use the highest available resolution; a legacy of spectroscopic research. Griffiths has shown that many practical laboratory problems of detection and recognition are much better off with a minimal resolution.[3]

Most organic molecules of interest in chemical defense have molecular weights greater than 100 and are asymmetrical; consequently, have no discernible fine structure[4]. The spectra of standard chemical agents[5,6] show bandwidths ranging from about 6 cm^{-1} to as much as 30 cm^{-1}. Some precursor compounds do exhibit fine structure[7], with bandwidths as low as 1.5 cm^{-1} at atmospheric pressure. There has been controversy over the best resolution to use for detecting compounds of these types in the atmosphere where bandwidths are as little as 0.1 cm^{-1}, the argument being that while low resolution may be adequate for the target much higher resolution is necessary to separate the target from the background. While an exact answer to this latter question is beyond the scope of this study, we will show that high resolution exacts a very high cost in sensitivity or signal to noise ratio (SNR).

There are two ways of looking at the detection and recognition problem: 1) conventional inspection combined with signal enhancement and quantification techniques and 2) automatic pattern recognition techniques[8,9,10,11,12,13] (artificial intelligence). The 2 methods are not mutually exclusive; in fact they can be used in tandem. However, it is safe to say that, to date, most practical field spectroscopy is accomplished by inspection.

For several reasons pattern recognition is likely to become a more important method for field detection problems: lower signal to noise spectra and much higher sensor data rates. It may be that threshold detection levels are not the same for inspection and pattern recognition or possibly not even the same resolution is optimally suitable for both tasks. Add to this that quantification - a very difficult problem for passive IR - is likely to depend optimally on resolution; low resolution causes deviation from linear behavior while high resolution increases noise. These questions will be addressed in future work. In this work, we shall explore the detectability of a target compound based on a single Lorentzian band of similar characteristics.

2. The Signal

The process of interest is detection of vapors in the open atmosphere by radiation transfer between a target vapor and a background. We will use the signal

model described by Flanigan and Walter[14]. The radiance of a layer of infinitesimal thickness dx is

$$dL = \alpha_T c_T L_{bg} \Delta\nu dx - \alpha_T c_T L_{amb} \Delta\nu dx \quad \iota_A c_A L_{bg} \Delta\nu dx - \alpha_A c_A L_{amb} \Delta\nu dx \qquad (1)$$

where α_T (m^2/mg) is the absorptivity due to the target, α_A is the absorptivity due to atmosphere, L_{bg} ($w/(cm^2\ sr\ cm^{-1})$) is the spectral radiance of a blackbody at the radiometric temperature of the background, L_{amb} is the radiance of a blackbody at the temperature of the layer and $\Delta\nu$ (cm^{-1}) is the optical resolution of the sensor. Assuming that atmospheric and target gases are uniformly distributed over the layer, eq 1 can be integrated over x to give the radiance incident on the sensor,

$$L_S = \tau_A \tau_T L_{bg} \Delta\nu + (1 - \tau_A \tau_T) L_{amb} \Delta\nu \qquad (2)$$

where τ_A is the atmospheric transmittance, and τ_T is the target gas transmittance. This is the simplest possible signal model that we can use for passive infrared detection. A more realistic model would consist of as many layers as needed to define the remote sensing problem of interest.

Passive IR detection depends on L_{amb} and L_{bg}[15]. Only a small fraction of the radiance incident on the sensor, L_S, contains useful information. This useful radiance, ΔL, can be determined by subtracting the ambient temperature spectral radiance and simplifying to give

$$\begin{aligned} \Delta L &= \tau_A \tau_T L_{bg} \Delta\nu + (1 - \tau_A \tau_T) L_{amb} \Delta\nu - L_{amb} \Delta\nu \\ \Delta L &= (1 - \tau_T \tau_A)(L_{amb} - L_{bg}) \Delta\nu \end{aligned} \qquad (3)$$

For the problems discussed here, the atmospheric transmittance will be assumed to be 1.

$$\Delta L = (1 - \tau_T)(L_{amb} - L_{bg}) \Delta\nu \qquad (4)$$

In the following section the emissivity of the ambient temperature blackbody will be defined by the emissivity of the gas using a band model.

2.1 The Lorentzian Band

The Lorentzian band is commonly used by spectroscopists to simulate real bands, both rotational lines[16] and vibrational bands for quantitative analysis[17]. In this model the absorptivity, α, of a Lorentzian band as a function of wavenumber is given by

$$\alpha(\nu) = \alpha_{pk} \frac{\gamma^2}{\gamma^2 + (\nu - \nu_0)^2} \qquad (5)$$

where α_{pk} is the peak absorptivity, gamma is the half width at half height, which is 1/2 the full width half height bandwidth (FWHH). A typical α_{pk} for compounds of interest ranges from 0.4 X 10^{-3} m^2/mgm to 1.5 X 10^{-3} m^2/mgm; we will use a convenient average of 10^{-3} m^2/mgm. For these preliminary investigations, we used 2 FWHHs: 1 cm^{-1} and 15 cm^{-1}. Figure 1 shows the profile of a 15 cm^{-1} band. (Most of the computing and graphics for this project were performed with Mathematica™[18].)

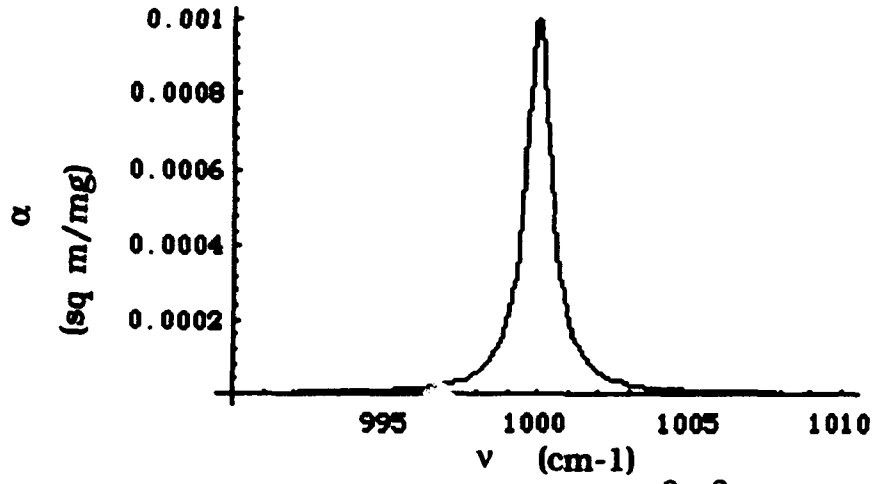

Figure 1. Profile of a 15 cm-1 band with a α_{pk} of 10^{-3} m^2/mg

Several techniques were used to study the effect of optical resolution on absorptivity coefficient, α, including: integration of the Lorentzian function to produce a closed form solution, and several numerical integration techniques. The closed form solution was particularly convenient to study signal to noise as a continuous function of resolution. The absorptivity coefficient, α, was averaged over a rectangular function of bandwidth, Δν. Integrating eq 5 and averaging by Δν

$$\bar{\alpha} = \frac{1}{\Delta\nu}\int_{\bar{\nu}_0}^{\Delta\nu/2} \alpha(\nu)d\nu = \frac{\alpha_{pk}}{\Delta\nu}\left(\gamma\, ArcTan\left(\frac{\nu-\nu_0}{\gamma}\right)\right) \qquad (6)$$

where the integration is carried out from ν_0 to $\Delta\nu/2$ because the integrand of the Lorentzian function is odd about ν_0. Figure 2 shows the average α as a function of increasing optical band for a 15 cm^{-1} band.

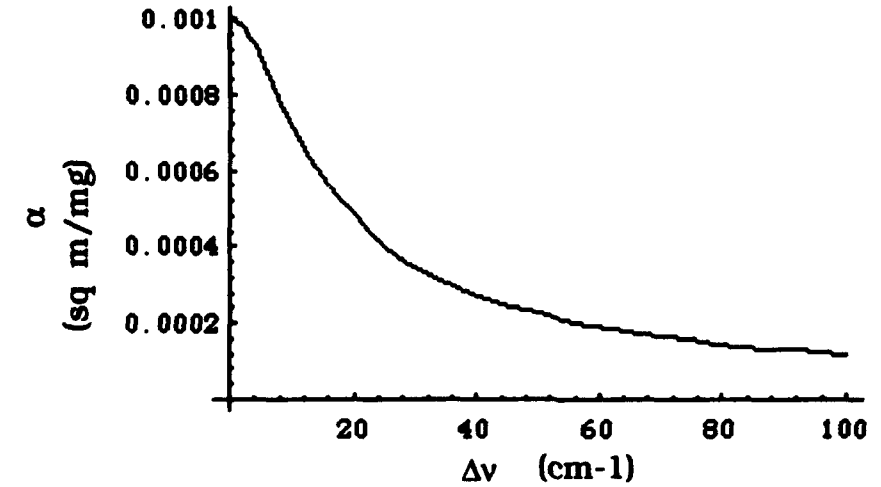

Figure 2. The average or effective α as a function of decreasing optical resolution (increasing optical bandwidth).

The optical signal incident on the sensor is now defined; we next pursue the signal to noise produced by the sensor.

2.2 Detector Limited Detection

Wolfe[19] gives an expression for the signal to noise ratio (SNR) of an extended source, detector-noise limited with the detector as field stop. That equation, after modification to our format, is

$$SNR_D = \int_0^{\Omega} (A_D)^{1/2} \cos\theta d\Omega \int^{\Delta\nu} \Delta f_\nu^{-1/2} \tau_s \frac{\Delta L_\nu}{\Delta\nu} D^* d\nu \qquad (7)$$

where

A_D is the area of the detector in cm^2,
θ is the angle of the ray with the optical axis,
$d\Omega$ is the solid angle,
Δf is the electronic bandwidth (Hz), which for Fourier transform spectrometers (FTS) is a function of ν,
τ_s is the sensor transmittance, and
D^* is the specific detectivity ($Hz^{1/2}$ cm/w)

The first integral is the étendue divided by $A_D^{1/2}$. Assuming that the variation of other quantities is small over the interval $\Delta\nu$

$$SNR_D = \frac{\tau_s \Im D^* \Delta L}{(A_D \Delta f)^{1/2}} \qquad (8)$$

The noise formulation is, to this point, applicable equally to either a filter or a FTS. Although results will be presented in wavenumber space, the intent is to define the performance of a FTS for which the electronic frequency is[20]

$$f = k\nu \qquad (9)$$

where k is the retardation rate (velocity of the mirror) The retardation, ΔX, required for resolution $\Delta\nu$ is

$$\Delta X = \frac{1}{\Delta\nu} \qquad (10)$$

If the scan is completed in t seconds, then the mirror velocity k is

$$k = \frac{\Delta X}{t} = \frac{1}{\Delta\nu\, t} \qquad (11)$$

Substituting these quantities into eq 9, the frequency becomes

$$f = k\nu = \frac{\nu}{\Delta\nu t} \qquad (12)$$

Usually, the signal is filtered on both the low frequency and high frequency sides. In the case of a single band system, the electronic frequency need only be as large as "audio" frequency bandwidth associated with the optical band. Remembering, of course, when the band is so limited. changes in the interferogram, other than random in-band noise, will cause changes outside the band (broadening, sidebands, etc). However, because the only noise accounted for in this study is random detector noise or BLIP noise it seems reasonable to limit the electronic bandwidth accordingly. Differentiating and setting $dv = \Delta v$

$$df = k\,dv = \frac{\Delta v}{\Delta v t} = \frac{1}{t} \tag{13}$$

Substituting eqs 4 & 13 into eq 8, the final SNR expression for a detector limited sensor is

$$SNR_D = \frac{\tau_S \Im D^* \Delta L t^{1/2}}{A_D^{1/2}}$$

$$SNR_D = \frac{\tau_S \Im D^* t^{1/2} \Delta v}{A_D^{1/2}} (1 - \tau_T \tau_A)(L_{amb} - L_{bg}) \tag{14}$$

2.3 Background Limited Incident Photon (BLIP) Detection

Photon noise limited detection is also known as shot noise and background limited incident photon (BLIP) noise or, more commonly, background limited detection. Background limited detection assumes a constant background; fluctuations are completely due to the probability of emission of a photon. Other fluctuations in the background contribute additional noise if the frequency of the fluctuations is within the electronic bandpass of the sensor and as mentioned above, can produce side bands at adjacent frequencies. The latter will be investigated in future work.

Several background limited models appear to give different results. These will be independently discussed.

2.3.1 Wolfe Model

Wolfe substitutes D^*_{BLIP} for D^* according to the relationship

$$D^*_{BLIP} = \left(\frac{\eta}{2Q_B}\right)^{1/2} \frac{1}{hcv} \tag{15}$$

where Q_B is the power spectrum of the variation in the number of photons incident per unit area. Kruse[21] shows that,

$$Q_B = 2\bar{n} = 2E_q \tag{16}$$

or the power spectrum of the variation is twice the average rate. It is also shown that the units of Q_B are the number of photons squared per unit area per second squared, per Hz and is numerically equal to twice the photon irradiance, E_q. Using these definitions, we can see that

$$E_q = \frac{E}{hcv} = \frac{1}{hcv} \frac{\tau_S \Im L_{bg} \Delta v}{A_D} \tag{17}$$

Substituting into eq 15,

$$D^*_{BLIP} = \left(\frac{\eta hc\nu A_D}{4\tau_s \Im L_{bg} \Delta\nu}\right)^{1/2} \frac{1}{hc\nu} = \left(\frac{\eta A_D}{4hc\nu\tau_s \Im L_{bg} \Delta\nu}\right)^{1/2} \qquad (18)$$

Detector limited sensors are limited by mechanisms internal to the detector; BLIP sensors are limited by the total amount of power reaching the detector. Increasing the bandwidth of a BLIP detector decreases the D^*. Figure 3 shows the decreasing D^* of a background limited detector as a function of optical bandwidth for a sensor with the specifications of the XM21. (See section 3.0.)

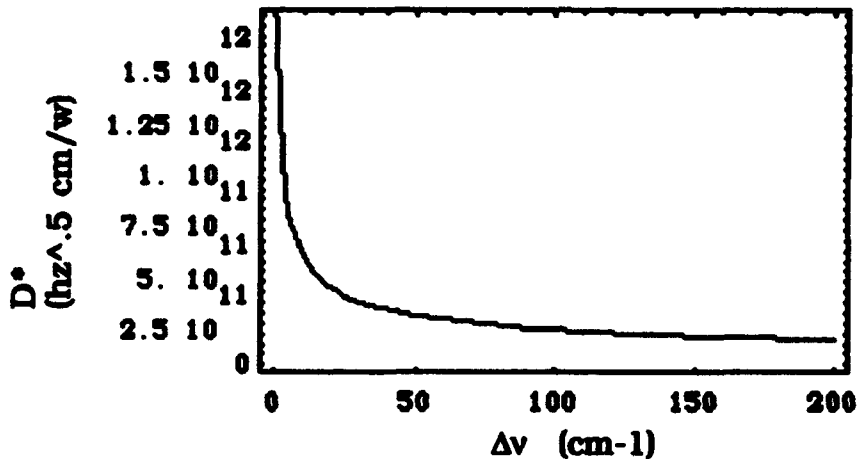

Figure 3. Background limited D^* as a function of spectral bandwidth.

For a 1 cm^{-1} total optical bandwidth BLIP sensor the D^*_{BLIP} would be about 1.6 x 10^{12}; for a BLIP sensor of optical bandwidth of 200 cm^{-1}, the D^*_{BLIP} would be about 1.2 x 10^{11} or about 6 times the specified $D^* \geq 2.8 \times 10^{10}$ for an XM21 (to be discussed).

Substituting eq 18 into eq 14, we get the background limited SNR based on Wolfe's model.

$$SNR^W_{BLIP} = \frac{\tau_s \Im \Delta L \Delta t^{1/2}}{A_D^{1/2}} \frac{(\eta A_D)^{1/2}}{(4hc\nu\tau_s \Im L_{bg} \Delta\nu)^{1/2}}$$

$$SNR^W_{BLIP} = \left(\frac{\eta \tau_s \Im t}{4hc L_{bg}}\right)^{1/2} \frac{\Delta L}{(\nu\Delta\nu)^{1/2}} \qquad (19)$$

$$SNR^W_{BLIP} = \left(\frac{\eta \tau_s \Im t}{4hc} \frac{\Delta\nu}{\nu}\right)^{1/2} (1 - \tau_T \tau_A) \frac{(L_{amb} - L_{bg})}{L_{bg}^{1/2}}$$

2.3.2 Kingston Model

Kingston defines the signal current as[22]

$$i_s = \frac{\eta e P_S}{hc\nu} = \frac{\eta e \Im \tau_S \Delta L}{hc\nu} \tag{20}$$

where η is the quantum efficiency of the detector; e is the electron charge, P_S is the power on the detector, τ_S is overall sensor transmittance, $\Im$ is the étendue, h is Planck's constant, c is the speed of light and ν is the wavenumber of the radiation detected.

For a constant background, the sensor will be "photon noise or background limited". Kingston bases his derivation of the mean square fluctuation of a number of Poisson distributed events as

$$\overline{(n-\bar{n})^2} = \overline{n^2} - \overline{2n\bar{n}} + \bar{n}^2 = \overline{n^2} - \bar{n}^2 = \bar{n} \tag{21}$$

Therefore, the mean square fluctuation of events is equal to the average number of events. (Note that Wolfe's derivation equates the photon variation to 2 times the average rate.) This observation leads to the following expression for the mean square fluctuation of the current.

$$\bar{i}_N^2 = 2ei\Delta f = \frac{2\eta e^2 \left(P_S + P_{bg}\right)\Delta f}{hc\nu} \tag{22}$$

where P_S and P_{bg} are the signal and background powers respectively. In this case $P_S \ll P_{bg}$, therefore the total background power is

$$P_{bg} \approx \tau_S \Im L_{bg} \Delta\nu \tag{23}$$

not including any instrument self emission. The mean square noise is

$$\bar{i}_N^2 = \frac{2\eta e^2 P_{bg} \Delta f}{hc\nu} = \frac{2\eta e^2 \tau_S \Im L_{bg} \Delta\nu \, \Delta f}{hc\nu} \tag{24}$$

Substituting for the bandwidth, equation 24 becomes

$$\bar{i}_N^2 = \frac{2\eta e^2 \tau_S \Im L_{bg} \Delta\nu}{hc\nu t} \tag{25}$$

Kingston defines the signal power to the noise power at the output of the integrating filter as the ratio of the square of the signal current to the mean square noise.

$$SNR_{BLIP}^K = \frac{i_S^2}{\bar{i}_N^2} = \left(\frac{\eta e \Im \tau_S \Delta L}{hc\nu}\right)^2 \frac{hc\nu t}{2\eta e^2 \tau_S \Im L_{bg} \Delta\nu} = \frac{\eta \Im \tau_S t \Delta L^2}{hc\nu L_{bg} \Delta\nu} \tag{26}$$

Substituting for ΔL the final form of the SNR expression based on the Kingston background limited model is

$$SNR_{BLIP}^K = \frac{\eta \Im \tau_S t}{hc} \frac{\Delta\nu}{\nu} (1-\tau_T)^2 \frac{(L_{amb} - L_{bg})^2}{L_{bg}} \tag{27}$$

Comparing eq 26 with eq 19

$$SNR^{W}_{BLIP} = \left(\frac{\eta \tau_s \Im t}{4hc}\frac{\Delta\nu}{\nu}\right)^{1/2}(1-\tau_T\tau_A)\frac{(L_{amb}-L_{bg})}{L^{1/2}_{bg}} \qquad (19)$$

we see that

$$SNR^{K}_{BLIP} = 4\left(SNR^{W}_{BLIP}\right)^2 \qquad (28)$$

The origin of this discrepancy is the definition of SNR. Kingston defines the SNR equals the square of the signal over the mean square of the noise and clearly supports this with "the output power from a photon detector, or any incoherent radiation detector, is proportional to the square of the input power". Additionally, Wolfe uses a statistical derivation that results in the variation in photon rate of twice the average rate, while Kingston's uses a derivation which results in the variation being equal to the average photon rate. The definition of SNR as the ratio of the power to the root mean square of the background fluctuations seems to be more widely accepted and the predictions more consistent with experience; therefore, we will use Wolfe's BLIP model (eq 19).

3. SNR For a Single Band

The XM21[23] specifications will be used to estimate the SNR by the D^* and D^*_{BLIP} models. An optical schematic for the XM21 is shown in figure 4.The estimated sensor transmittance is 0.38 based on: entrance window (.93), scanning mirror (.99), Beam splitter (.48), retro mirror (.99), exit lens (.97), lens window (.97), and field lens (.97). These estimates were arrived at from the technical specifications and some extrapolation between similar parts. The étendue of the XM21 is 0.0029 cm^2 sr and the detector size is 0.07 cm on a side.[24] The D^* for the XM21 is specified to be not less than 2.8×10^{10} $Hz^{1/2}$ cm/w between 1250 and 785 cm^{-1}

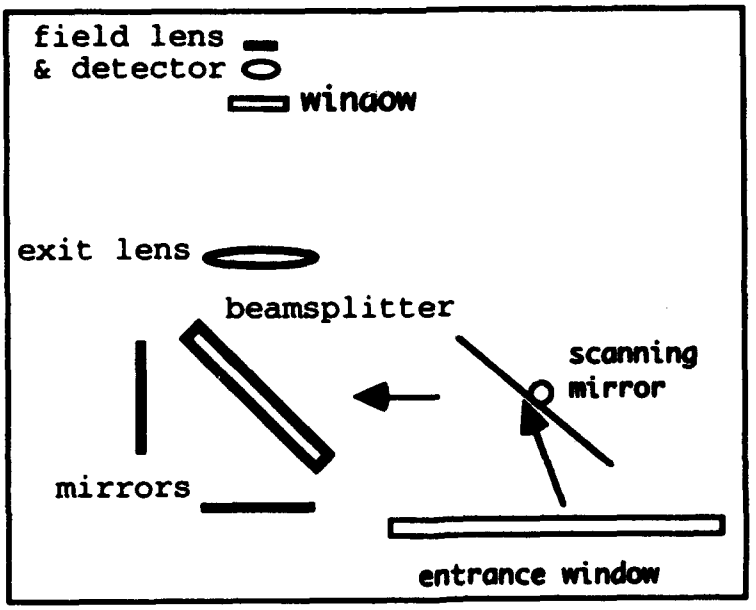

Figure 4. A schematic of the XM21, a typical remote FTS without a telescope.

Figure 5 shows the SNR for these values for D^* limited detection for a 1 cm^{-1} band FWHH with α_{pk} = .001 m^2/mg located at 1000 cm^{-1}. The background

temperature was 300 °K and the ambient temperature was 301 °K for a ΔT of -1 °K. All parametric studies unless otherwise stated were conducted at 3 scan times of 0.1 sec, 1.0 sec and 10 seconds. The CL = 50 mg/sq m, which produces about 5% absorption (95% transmittance). Figure 6 is SNR for a 15 cm^{-1} band; all other values were the same.

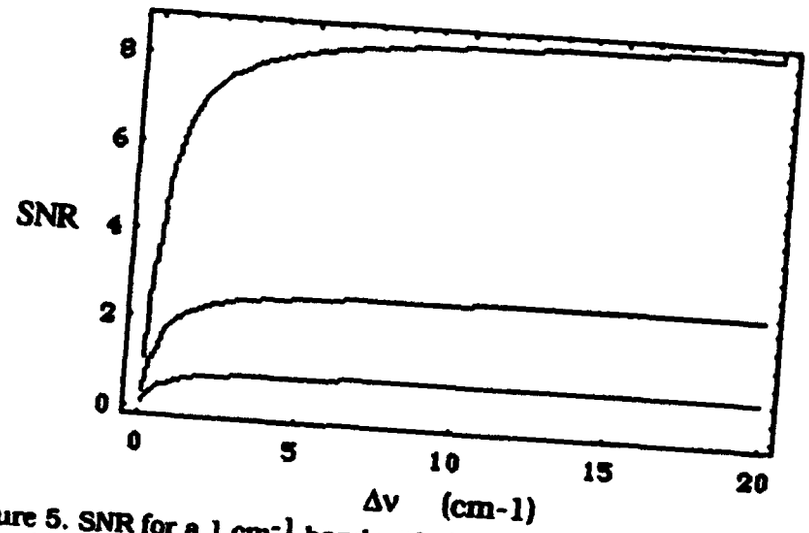

Figure 5. SNR for a 1 cm^{-1} band with detector limited detection, 3 measurement times: top = 10 sec, middle = 1.0 sec, and bottom = 0.1 sec.

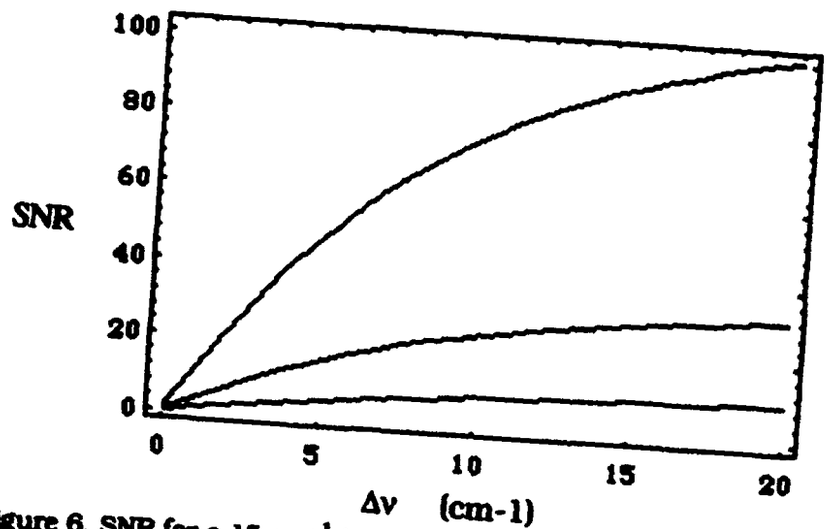

Figure 6. SNR for a 15 cm^{-1} band with detector limited detection

SF_6 is a commonly used simulent for field testing of passive IR sensors because of its innocuous nature and a very strong spectral band at 947 cm^{-1}. Based on spectral data given in reference 7 and methods of conversion described in reference 4, α_{pk} has a value of 1.15×10^{-2} sq m/mg. This is about 1/2 the bandwidth and 14 times the intensity of an average organophosphorous band. Figure 7 shows SNR for a Lorentzian band of similar properties and an assumed CL of 50 mg/sq m (about 56% transmittance).

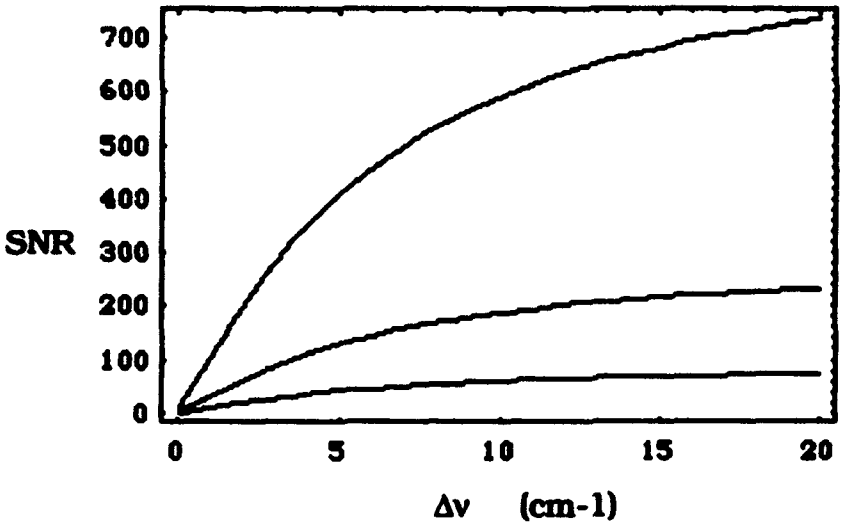

Figure 7. SNR for SF_6 with detector limited detection.

Table 1 shows comparative SNRs for the 3 bands at 1 sec scan time from figures 5, 6, and 7.

Δv	1 cm^{-1} band	15 cm^{-1} band	8.8 cm^{-1} band
2	2.3	6.8	62
4	2.5	13	110
8	2.7	21	170
16	2.73	30	220

Table 1. SNR for 1 sec scan time for detector limited detection. ΔT = -1 °K, CL = 50 mg/m^2. Values taken from figures 5, 6 & 7.

From Table 1, we conclude that the SNR improves at higher optical bandwidths, i.e., lower resolution for characteristic broad bands. For the 1 cm^{-1} band the improvement occurs at lower increases in resolution. For optical resolutions in the range of 0.2 cm^{-1} the SNR is marginal for all scanning times. For this detector limited model the SNR continues to improve with increases in optical bandwidth; the limit will be imposed by other conditions including band separation in a multiband environment. Another observation is: that while the SNR continues to improve with increasing optical bandwidth, increasing the bandwidth does not compensate for short measurement times.

Figures 8, 9, and 10 give the SNR for background limited (BLIP) sensors for the same conditions shown in figures 5, 6, and 7.

The most notable differences between detector limited and background limited cases are the vastly higher sensitivities of the background limited case and the appearance of optima in the background limited case. Table 2 shows the peak SNR, the fractional bandwidth for each peak and the SNRs for the background limited case for the 1 sec scan time taken from figures 8, 9, & 10. The optimal SNR occurs at 75% of the bandwidth. This is, of course, only for the BLIP case.

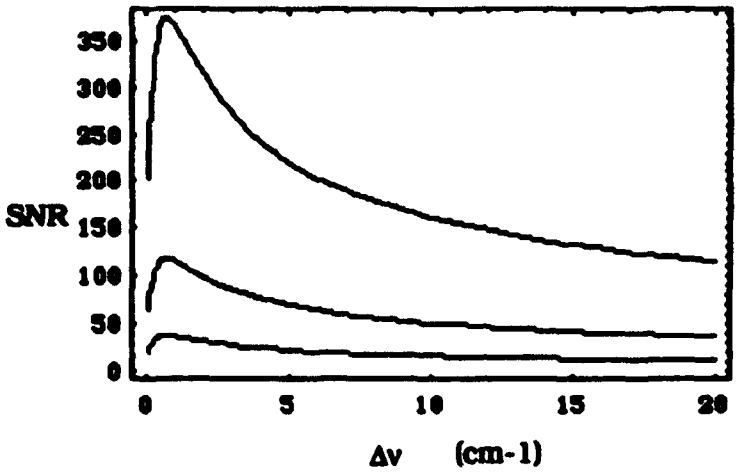

Figure 8. SNR for a 1 cm^{-1} band for background limited detection.

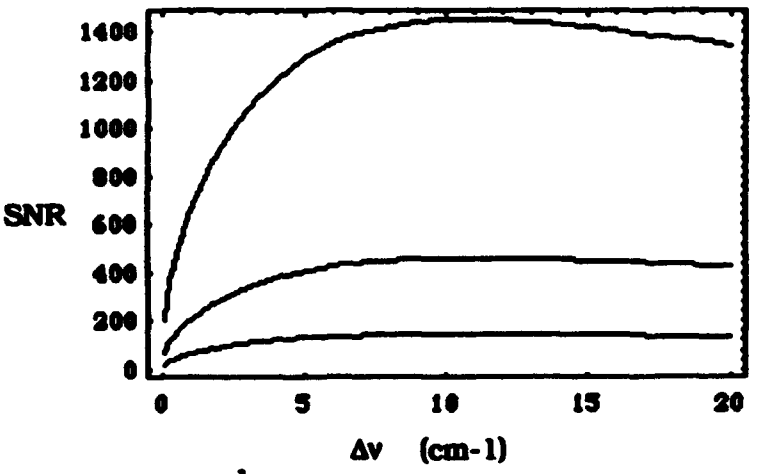

Figure 9. SNR for a 15 cm^{-1} band for background limited detection

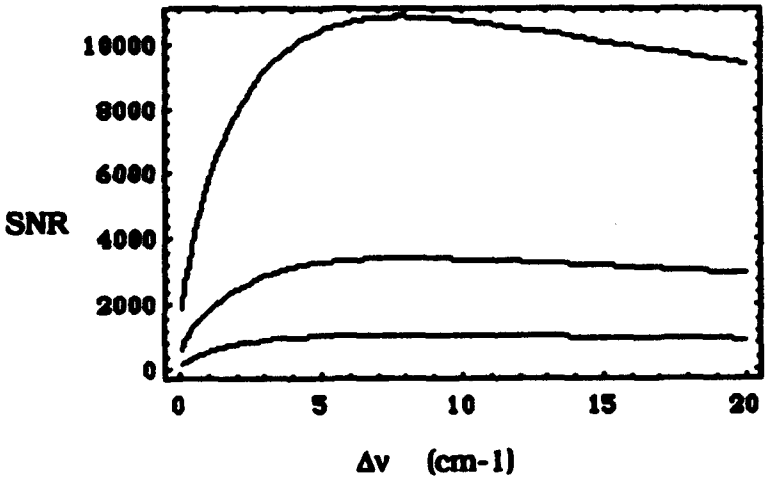

Figure 10. SNR for SF_6 for background limited detection.

Δv	1 cm^{-1} band	15 cm^{-1} band	8.8 cm^{-1} band
peak	0.71	10.5	7.76
peak/Δv	0.71	0.71	0.88
SNR	119	460	3420

Table 2. Optimum resolution and SNR for 1 sec scan time for background limited detection. ΔT = -1 °K, CL = 50 mg/m^2. Values taken from figures 8, 9, & 10.

3.1 Noise Equivalent Concentration Pathlength (NECL)

The NECL can be obtained by setting SNR to 1 in eq 14 and solving for CL.

$$NECL = \frac{1}{\alpha} \ln \left[\frac{1}{1 - \left(\frac{A_D^{1/2}}{\tau_s \Im D^* \Delta \nu t^{1/2} \left(L_{amb} - L_{bg} \right)} \right)} \right] \qquad (29)$$

Figure s 11, 12, & 13 show NECL as a function of Δv for a detector limited sensor and 1 cm^{-1}, 15 cm^{-1}, and SF_6 bands respectively. These curves illustrate how rapidly threshold sensitivity levels improve with modest increases in optical bandwidth in the region around the width of the target bands. Notice also that threshold concentration approaches a constant value more quickly than does the SNR.

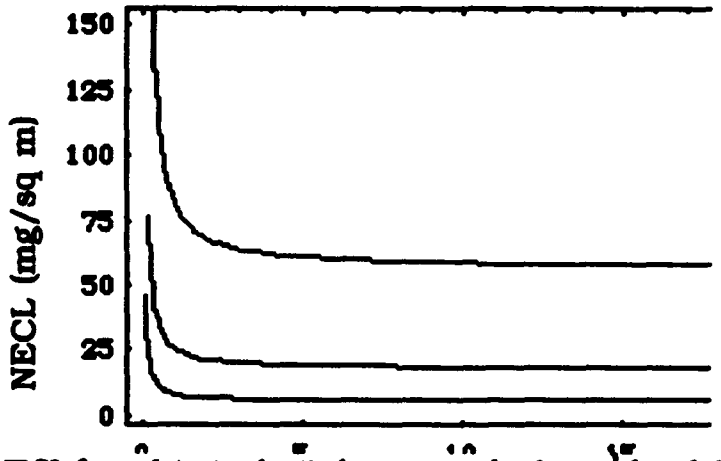

Figure 11. NECL for a detector limited sensor and a 1 cm^{-1} band. Note that the order of sensitivity is reversed compared to the SNR figures. The scanning times are from top to bottom: t = 0.1 sec, t = 1.0 sec, and t = 10 sec with the most sensitive (10 sec) being at the bottom.

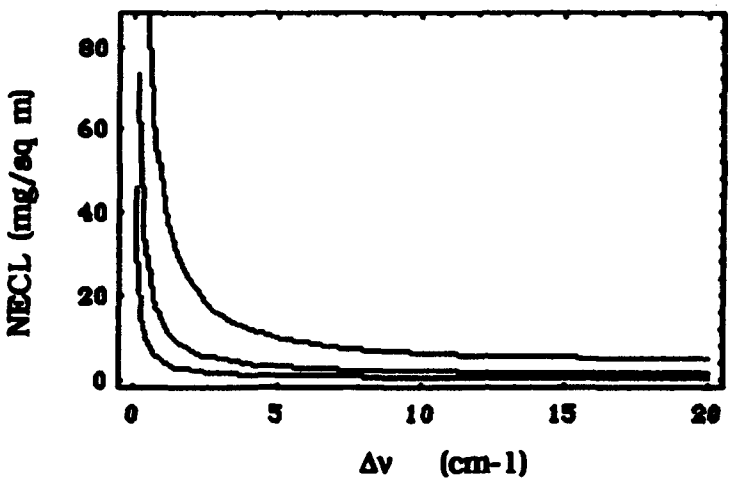

Figure 12. NECL for a detector limited sensor and a 15 cm^{-1} band.

The background limited NECLs can be computed from eq 29 with the BLIP D^* (eq 19) substituted for the measured D^*. Figures 14, 15 and 16 show NECLs for the same targets and the same conditions for a background limited sensor.

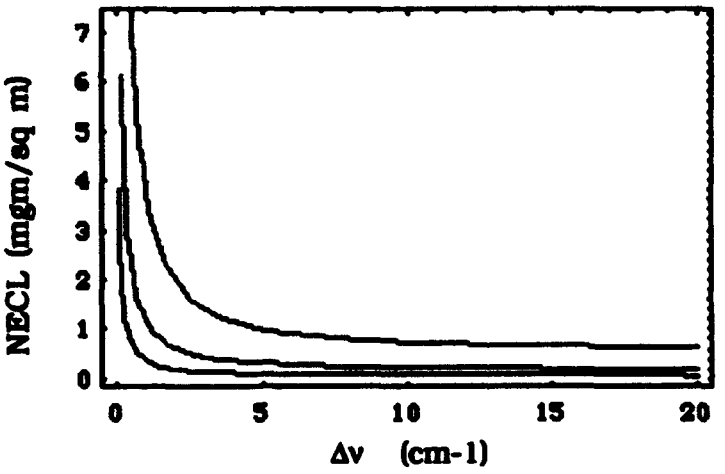

Figure 13. NECL for the 8.8 cm^{-1} (SF_6) and a detector limited sensor

Δv	1 cm^{-1} band	15 cm^{-1} band	8.8 cm^{-1} band
2	21	6.8	0.6
4	19	3.8	0.36
8	18	2.3	0.27
16	18.6	1.9	0.20

Table 3. Comparative NECLs for 1 sec scan time for detector limited detection. ΔT = -1 °K. Data taken from figures 11, 12, & 13.

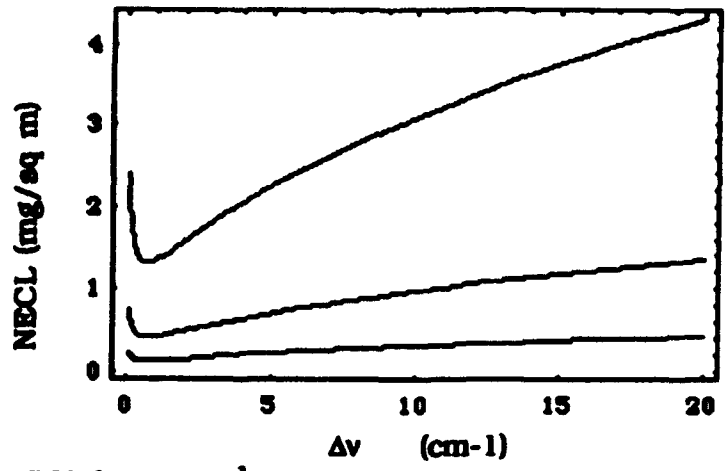

Figure 14. NECL for a 1 cm^{-1} band and a background limited sensor

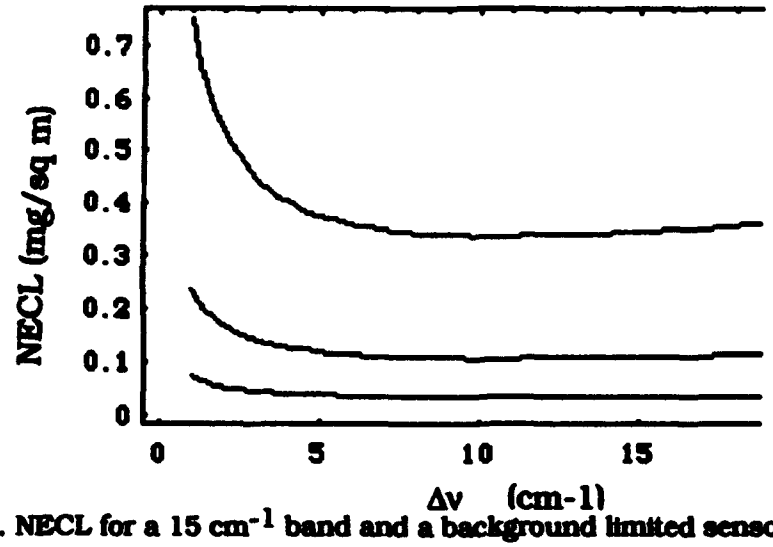

Figure 15. NECL for a 15 cm^{-1} band and a background limited sensor

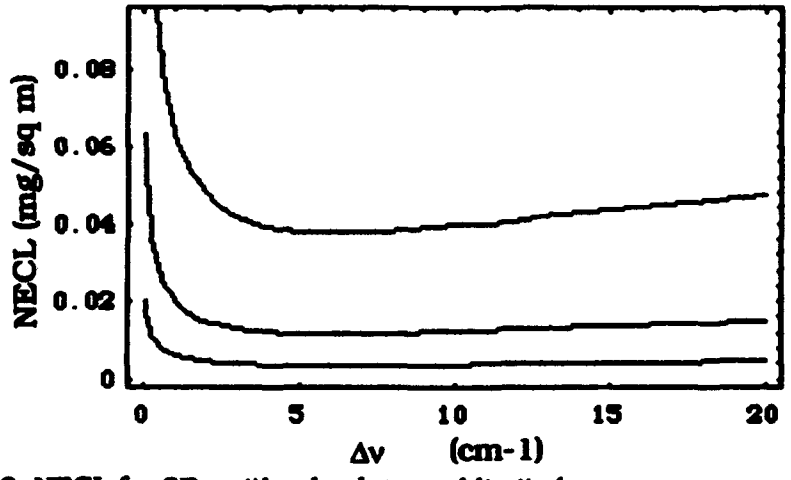

Figure 16. NECL for SF_6 with a background limited sensor

Δν	1 cm^{-1} band	15 cm^{-1} band	8.8 cm^{-1} band
2	0.50	0.17	0.015
4	0.65	0.13	0.012
8	0.88	0.10	0.012
16	1.2	1.2	0.014

Table 4. Comparative NECLs for 1 sec scan time for background limited detection. ΔT = -1 °K. Values taken from figures 14, 15, and 16.

Again, the background limited cases show well defined optima, minima in this case when compared to the detector limited case.

3.2 Noise Equivalent Δ Temperature (NEDT)

The NEDT can be obtained by setting SNR to 1 in eq 13 and solving for the background temperature and subtracting that from the ambient temperature.

$$NEDT = \frac{c_2 \nu}{Ln\left(1 + \frac{c_1 \nu^3}{\left(L_{amb} - \frac{A_D^{1/2}}{\tau_s \Im D^* \Delta\nu\, t^{1/2}(1-\tau_T)}\right)}\right)} - T_{amb} \qquad (30)$$

where c_1 and c_2 are coefficients in the Planck equation ($c_1 = 1.19 \times 10^{-12}$ and $c_2 = 1.4388$ for the units used in this study.) Eq 28 does not have solutions at all values of Δν; therefore the range has to be determined.

Figures 17 - 22 show the NEDT's for the 1 cm^{-1}, 15 cm^{-1}, and SF_6 bands for detector limited and background limited cases. CL = 50 mg/m^2 in all cases. Again, as for the other BLIP cases background limited D^* was substituted for measured D^*.

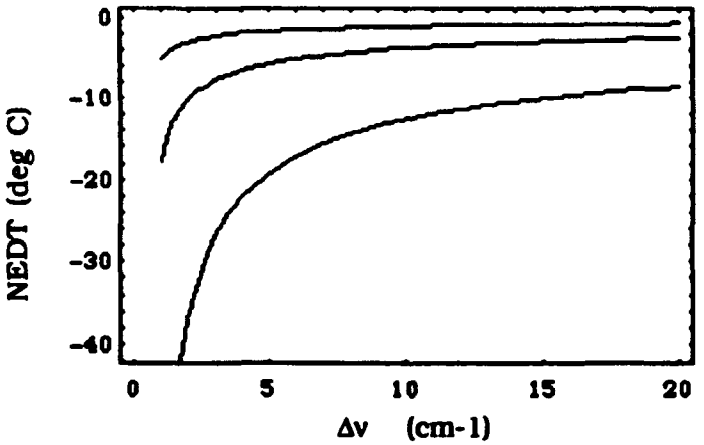

Figure 17. NEDT for a detector limited sensor and a 1 cm^{-1} band. The scanning times are from bottom to top: t = 0.1 sec, t = 1.0 sec, and t = 10 sec. The highest sensitivity is at the top.

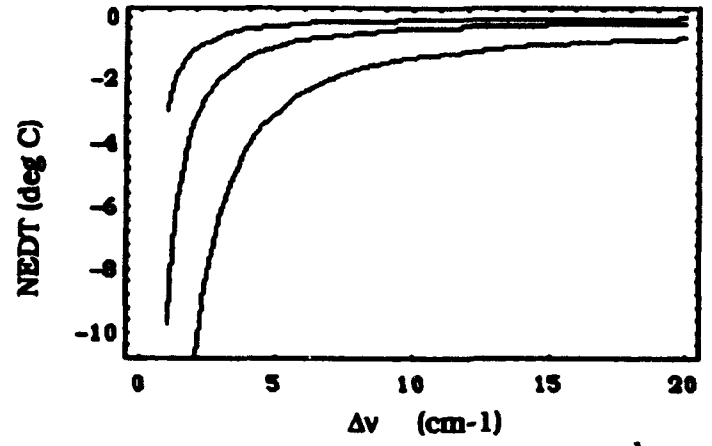

Figure 18. NEDT for a detector limited sensor and a 15 cm^{-1} band

For all bands the greatest improvements take place in the region below 4 cm^{-1}; for the 1 cm^{-1} band below 1 cm^{-1} bandwidth. However, for the broader bands there are still gains of 2 or more in going from 4 to 8 cm^{-1}. for the detector limited case. For broader bands there will additional gains.

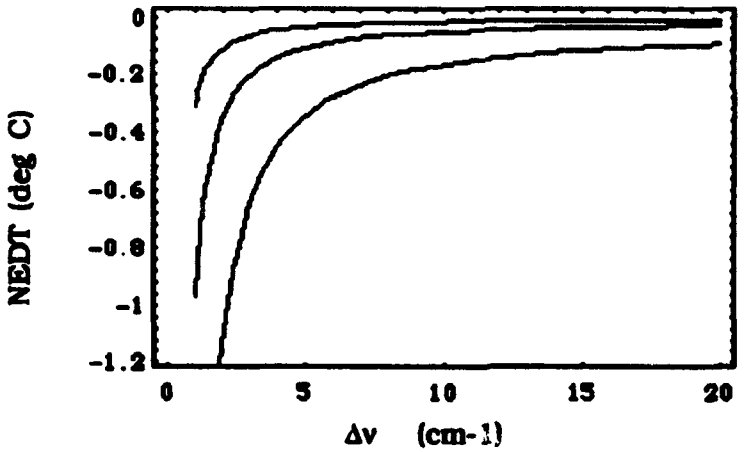

Figure 19. NEDT for a detector limited sensor and a 8.8 cm^{-1} band with α_{pk} = 0.0115.

Δv	1 cm^{-1} band	15 cm^{-1} band	8.8 cm^{-1} band
2	-0.44	-0.16	-0.015
4	-0.40	-0.074	-0.010
8	-0.34	-0.047	-0.005
16	-0.34	-0.034	-0.004

Table 5. Comparative NEDTs for detector limited detection. CL = 50 mg/m^2. Taken from figures 17, 18, & 19 for the 1 sec scan.

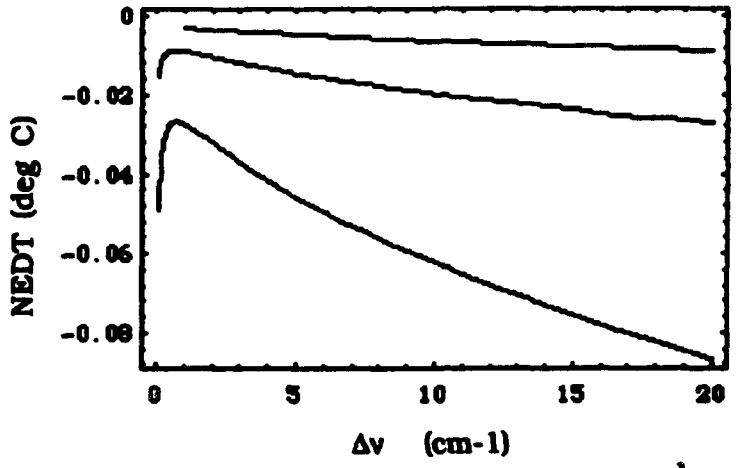

Figure 20. NEDT for a background limited sensor and a 1 cm^{-1} band

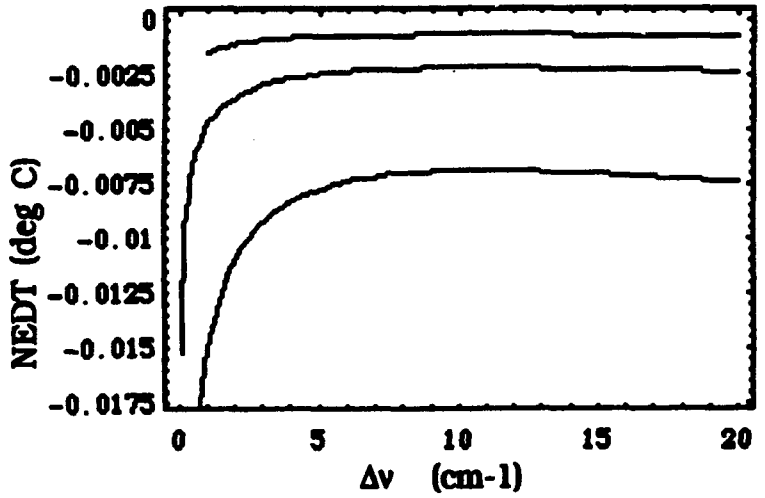

Figure 21. NEDT for a background limited sensor and a 15 cm^{-1} band

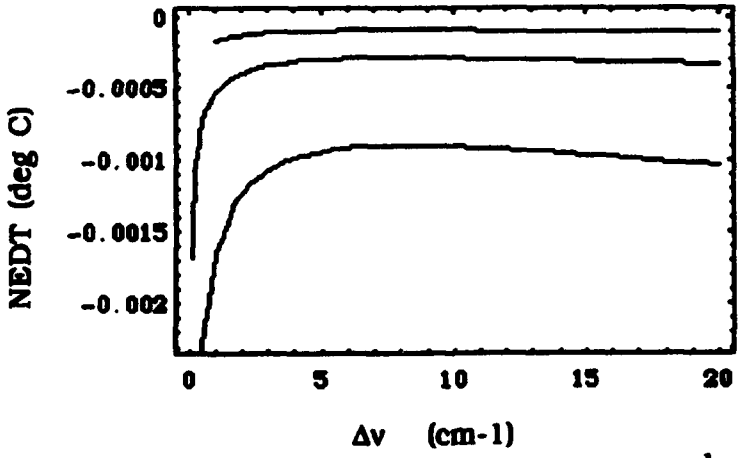

Figure 22. NEDT for a background limited sensor and a 8.8 cm^{-1} band

$\Delta\nu$	1 cm^{-1} band	15 cm^{-1} band	8.8 cm^{-1} band
2	-0.010	-0.0036	-0.00040
4	-0.013	-0.0026	-0.00031
8	-0.018	-0.0022	-0.00029
16	-0.025	-0.0022	-0.00031

Table 6. Comparative NEDTs for background limited detection. CL = 50 mg/m^2. Taken from figures 20, 21, & 22 for the 1 sec scan.

4. Summary and Conclusions

The objective of this effort was twofold: to begin the development of a computer model for passive infrared (IR) remote sensing vapor detection systems and to provide guidance in the determination of optimum spectral resolution for the remote detection of organic vapors. The target compounds were modeled as Lorentzian bands; this allowed a fairly simple analytical approach. Several sensor models were compared including: a detector limited sensor model according to Wolfe, and 2 background limited incident photon (BLIP) models based on work by Wolfe and Kingston. Measures of sensitivity were developed including: signal to noise ratio (SNR), noise equivalent concentration/pathlength (NECL), and noise equivalent ΔT (NEDT); all as a function of optical bandwidth. SNR, NECL and NEDT values were computed for a typical broad and narrow bands associated with organophosporous compounds at 3 scan times of: 0.1, 1.0 and 10 seconds. Additionally, the simulant, sulfur hexafluoride (SF_6) was evaluated.

It has been accepted for many years that modest resolutions are more effective for passive IR detection of organic vapors. This study quantifies that relationship for the first time. For problems where the ΔT and/or CL are small there may be additional gains of 2 to 5 in sensitivity by increasing optical bandwidth from the present standard of 4 cm^{-1} to 8 cm^{-1} or even 16 cm^{-1} resolution; although, this conclusion needs further study to insure that it does not introduce increased discrimination problems.

It is clear that present systems are limited by detector technology. With true background limited performance and careful optimization to a particular problem, sensitivity improvements of up to 50 may be possible.

This study is based on using the narrowest possible electronic bandwidth a condition which assumes that there are no fluctuations in the background other than shot noise. Consequently, the SNRs are probably unrealistically high for a multiband system.; it is the relative improvements that are of significance.

The next step in the development of the computer model is to develop the discrete spectral data base and synthesize noisy realistic spectra. Beyond that multiple layer models, with target and atmospheric transmittance, will be developed. Finally, these layers will be embedded in large scale codes such as DIRSIG.

References

[1] Barnett, B. W., Smith, B. T., & Stockum, L. A., "XM21 Background Characterization" Final Report DLA 900-86-C2045, Task 394, Battelle, 505 King Ave, Columbus, Ohio 43201-2693

[2] "Chemical Agent Warning and Detection Studies", Final Report, contract DA 18-035-AMC-104(A), Melpar, Inc. (1965)

[3] Griffith's, Peter R., FT-IR Spectrometry at Low Resolution: How Low Can You Go?, 9th International Conference on Fourier Transform Spectroscopy, Calgary, Alberta, Canada, Aug 23-27 1993

[4] Flanigan, D. F., The Spectral Signatures of Chemical Agent Vapors and Aerosols, CRDC-TR-85002, April 1985.

[5] Barrett, W.J., & Dismukes, E. B., "Infrared Spectral Studies of Agents and Field Contaminants, First Annual Report", Contract DAAA15-68-C-0154, Jan 31, 1969.

[6] Barrett, W.J., & Dismukes, E. B., "Infrared Spectral Studies of Agents and Field Contaminants, Second Annual Report", Contract DAAA15-68-C-0154, Dec 12, 1969.

[7] Infrared Analysis Inc. Data Base of Infrared Spectra of the NTS Chemicals.

[8] Kroutil, R., Combs, R., Knapp, R., and Small, G., "Remote Infrared Vapor Detection of Volatile Organic Compounds", 9th International Conference on Fourier Transform Spectroscopy", Calgary, Alberta Canada, (1993)

[9] Small, G.W., T. F. Kaltenbach, and R. T. Kroutil, Rapid Signal Processing Techniques for Fourier Transform Infrared Remote Sensing, Trends in Analytical Chemistry, Vol. 10, No. 5, May 1991.

[10] Small, G., Harms, A., Kroutil, R., Ditillo, J., Loerop, W., "Design of Optimized Finite Impulse Response Digital Filters for Use with Passive Fourier Transform Infrared Interferograms, Analytical Chemistry, 62, 1770 (1990)

[11] Small G.W., Kroutil, R.T., Ditillo, J.T., and Loerop, W., Detection of Atmospheric Pollutants by Direct Analysis of Passive Fourier Transform Infrared Interferograms, Analytical Chemistry, 60, No. 3, 1 February 1988.

[12] Kaltenbach, T.F., and Small, G.W., Development and Optimization of Piece wise Linear Discriminants for the Automated Detection of Chemical Species, Analytical Chemistry, 63, No. 9, 1 May 1991.

[13] Small, G.., Kroutil, R., Ditillo, J., Loerop, W., "Detection of Atmospheric Pollutants by Direct Analysis of Passive Fourier Transform Infrared Interferograms", Anal Chem, 60, 264, (1988)

[14] Flanigan, D. F., and Walter, H. Jr., The Computer Simulation and Optimization of Passive LOPAIR, ED-TR-74070, January 1975.

[15] Flanigan D.F., Detection of Organic Vapors with Active and Passive Sensors: A Comparison, Apl. Opt.. 25, pp. 4253-4260 (1986).

[16] Beer, R., "Remote Sensing by Fourier Transform Spectrometry", pg 49, John Wiley & Sons, (1992)

[17] Griffiths, P. R., de Haseth, J. A., Fourier Transform Infrared Spectrometry, pg 363, John Wiley & Sons, (1986)

[18] Wolfram, S., "Mathematica, "A System for Doing Mathematics by Computer", Addison Wesley Publishing Co, Inc, (1991)

[19] Wolfe, W. L., "Imaging Systems", The Infrared Handbook, Revised Edition, pg 19-6, 1985, ed by Wolfe and Zissis

[20] Griffiths, P. R., de Haseth, J. A., pg 9,

[21] Kruse, P. W., McGlauchlin, R., & McQuistan, R. B., Elements of Infrared Technology, John Wiley and Sons, New York, NY, 1962, pg 58

[22] Kingston, R.H., "Detection of Optical and Infrared Radiation", pg 15, Springer Verlag, (1978)

[23] XM21 Remote Sensing Chemical Agent Alarm (RSCAAL) Final Scientific and Technical Report, Prepared by Brunswick Defense, Deland, FL, Sept., 1990, for CRDEC-AMCCOM, Contract No. DAAK11-85-C-0015.

[24] Flanigan, D. F., "Chamber Optics for Testing Passive Remote Sensing Vapor Detectors", ERDEC-TR-127, Nov 1993